JOC The Journal of Organic Chemistry

Article

pubs.acs.org/joc

Fluorescent Acridine-Based Receptors for $H_2PO_4^-$

Vicente Martí-Centelles,[†,‡] M. Isabel Burguete,[†] Francisco Galindo,[†] M. Angeles Izquierdo,[†] D. Krishna Kumar,[‡] Andrew J.P. White,[‡] Santiago V. Luis,*[,†] and Ramón Vilar*[,‡]

[†]Department of Inorganic and Organic Chemistry, Universitat Jaume I, E-12070 Castellón, Spain

[‡]Department of Chemistry, Imperial College London, London SW7 2AZ, U.K.

Supporting Information

ABSTRACT: Two new pseudopeptidic molecules (one macrocyclic and one open chain) containing an acridine unit have been prepared. The fluorescence response of these receptors to a series of acids was measured in $CHCl_3$. Receptors are selective to $H_2PO_4^-$ versus HSO_4^-, and an even higher selectivity is found over other anions such as Cl^-, Br^-, CH_3COO^-, and CF_3COO^-. We show that the macrocyclic receptor is more selective for $H_2PO_4^-$ than the related open chain receptor. The supramolecular interactions of triprotonated receptors with different anions have been modeled in silico and have been studied by different experimental techniques. Optimized geometries obtained by computational calculations agree well with experimental data, in particular fluorescence experiments, suggesting that the selective supramolecular interaction takes places through coordination of the anions to the triprotonated form of the receptor.

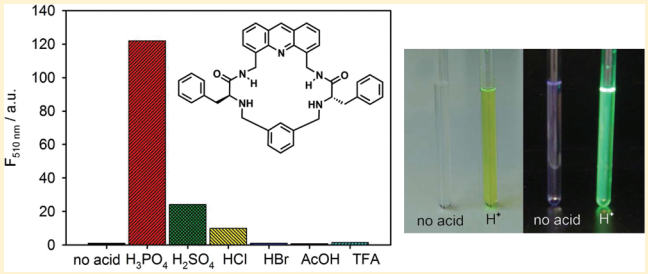

INTRODUCTION

Fluorescent receptors have important applications in a wide range of areas such as supramolecular, synthetic, bioorganic, medicinal, and biological chemistry.[1−14] Processes such as protein binding to specific ligands or molecular recognition of DNA can be studied with the help of fluorescent systems.[15−20] The recognition of acids is an interesting field that has been widely investigated.[21−32] However, in most cases, the recognition event is based on the interaction between the hydrogen ions generated upon acid dissociation and the molecular receptor. A direct and specific interaction of the receptor with the corresponding conjugate base is often lacking in the recognition process. In those cases, Coulombic interactions are predominant and a poor selectivity is generally found, usually with the recognition of the species having the highest charges.[33−35]

Chemical receptors containing acridine fragments have attracted interest due to the luminescent properties of this species. For example, some macrocyclic and open chain structures containing the acridine scaffold have been found to bind to DNA.[36,37] On the other hand, Kim et al. have prepared an imidazolium acridine derivative as a fluorescent chemosensor for pyrophosphate and dihydrogen phosphate.[38]

In recent years, some of us have focused on the preparation and study of pseudopeptidic macrocyclic structures. A central concept for the development of these compounds is the generation of well-defined three-dimensional multifunctional structures allowing them to selectively host small molecules and ions.[39−44]

In this paper, we report on the synthesis of two pseudopeptidic compounds, **1** and **2** (Chart 1), containing a functionalized acridine moiety and their fluorescence response to a series of acids in $CHCl_3$. These results show that both receptors are able to selectively recognize $H_2PO_4^-$ over other anions, with the macrocycle **2** being more selective for this anion than the open-chain compound **1**.

RESULTS AND DISCUSSION

Synthesis of the Receptors. Receptors **1** and **2** contain amide and amine groups that can interact with anions via hydrogen bonding and, if the amine is protonated, also via ion-pairing.[45,46] On the other hand, the acridine unit provides the compounds with fluorescent properties, and additionally, its protonation at the heterocyclic nitrogen atom can be used to add additional interactions with anions and regulate the fluorescent behavior of the system. Finally, the macrocyclic structure in compound **2** can provide an appropriate scaffold for a proper preorganization that can result in enhanced recognition properties.[47−51]

Receptors **1** and **2** were prepared as shown in Scheme 1. The 4,5-bis(aminomethyl)acridine dihidrochloride **3** was prepared according to previously reported procedures.[52] Pseudopeptidic compound **5** was obtained by reaction of 4,5-bis(aminomethyl)-acridine with the corresponding amino acid activated as its hydroxysuccinimide ester using dimethoxyethane (DME) as solvent. Best results were obtained when the reaction was stirred for 8 h at room temperature and then for 5 h at 50 °C. The Cbz protecting group was then removed with the use of HBr/AcOH to afford the amine hydrobromide, from which the

Received: October 11, 2011
Published: November 11, 2011

   dx.doi.org/10.1021/jo202077v | J. Org. Chem. 2012, 77, 490−500

Chart 1. Pseudopeptidic Receptors Containing Acridine Fragments Considered in This Work

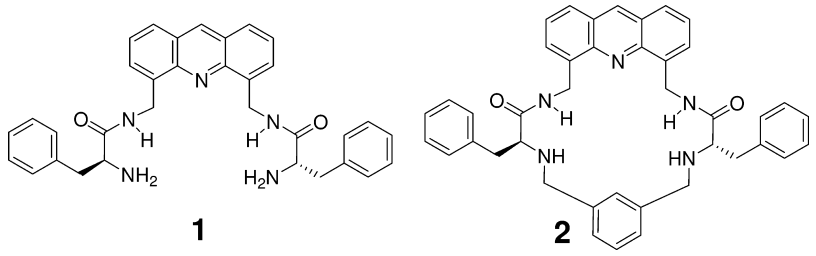

Scheme 1. Synthesis of Pseudopeptidic Receptors 1 and 2[a]

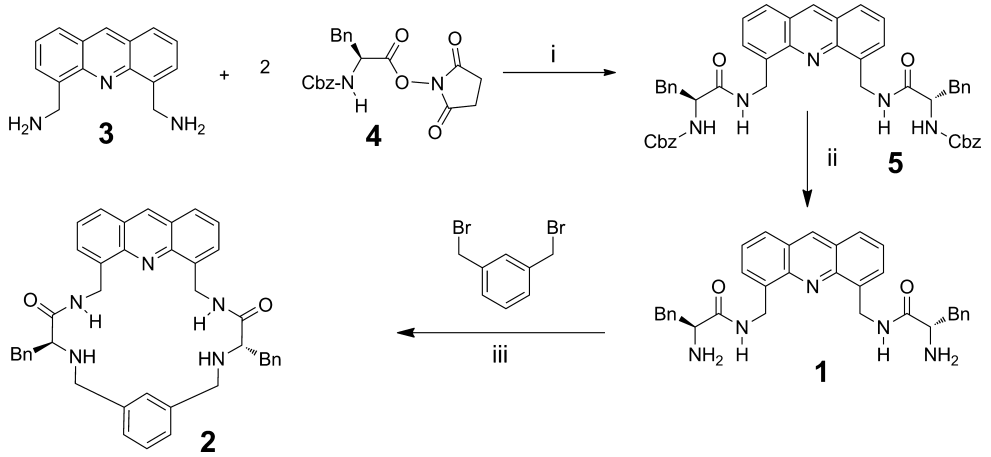

[a]Key: (i) DME, rt; (ii) HBr/AcOH 33%, rt then aq NaOH; (iii) TBABr, DIPEA, CH_3CN, temperature gradient from 50.0 to 81.6 °C.

free amine (open-chain receptor **1**) was obtained upon neutralization with NaOH. The key step for the preparation of macrocycle **2** was the final macrocyclization reaction. In this case, a careful control of the temperature with a temperature gradient, using conditions similar to those previously reported for related pseudopeptidic macrocycles,[53] provided significantly better yields than when the reaction was performed at reflux. Thus, macrocycle **2** was prepared from the reaction of bis(amidoamine) **1** with 1,3-bis(bromomethyl)benzene in CH_3CN, in the presence of tetrabutylammonium bromide (TBABr) and *N,N*-diisopropylethylamine (DiPEA), using a temperature gradient from 50.0 to 81.6 °C. The crude product was purified by column chromatography to afford the expected macrocycle in 85% yield. To the best of our knowledge, the preparation of pseudopeptidic structures containing acridine fragments has not been reported previously. It is clear that the relatively high yields obtained for the macrocyclization reaction involve a high degree of preorganization of the open-chain intermediate and the corresponding transition state, as has been demonstrated in other cases using this methodology[54−57] and open the way for the preparation of new families of macrocyclic receptors containing this important moiety.

Compounds **1** and **2** were characterized by spectroscopic and analytical techniques. Interestingly, in $CDCl_3$ solution, the ^1H NMR signals of the CH_2 groups at positions 4 and 5 of the acridine moiety are considerably different between compounds **1** and **2**. In the open-chain derivative **1**, these protons appear as doublets, whereas in compound **2** they appear as double doublets. This suggests the presence of an appreciable coupling constant with the amide hydrogen atom in **2** because of the higher rigidity provided by the macrocyclic structure.

Fluorescence Response to Acids. The electronic absorption spectra and the steady-state fluorescence emission spectra of **1** and **2** were recorded in $CHCl_3$. As expected,[58] compounds **1** and **2** have similar properties and both show absorption maxima at 357 nm and present a maximum of emission at 420 nm when excited at 357 nm (Figure 1).

Different experiments were carried out to analyze the potential interaction of both receptors with acids in $CHCl_3$. Thus, the interactions with H_3PO_4, H_2SO_4, HCl, HBr, acetic acid, and trifluoroacetic acid in $CHCl_3$ were studied. As can be seen in Figure 2, upon addition of acids there is an increase of emission in the case of H_3PO_4, which is more significant than in the case of H_2SO_4. The response toward HCl, HBr, acetic acid, and trifluoroacetic acid is practicably negligible. It must be noted that the recorded fluorescence corresponds to a new band centered at 510 nm, whereas the original fluorescence at 420 nm disappears when the new compound is formed. Titration fluorescence spectra did not show an isosbestic point, and therefore curves did not allow us to calculate the corresponding binding constants (see the Supporting Information). The much larger emission enhancement observed for H_3PO_4 suggested that compound **2** could be used as potential fluorescent chemical sensor for the detection of this acid.[59−67]

This is more clearly highlighted when the normalized emission values for the maxima of the corresponding emission bands are represented for both compounds. Figure 3 compares the fluorescence measured after the addition of 25 equivalents of each acid. We can see that both the open chain and the macrocyclic compound display preferred recognition toward H_3PO_4, being the affinity toward this acid higher with the macrocyclic receptor **2**.

dx.doi.org/10.1021/jo202077v | *J. Org. Chem.* 2012, 77, 490−500

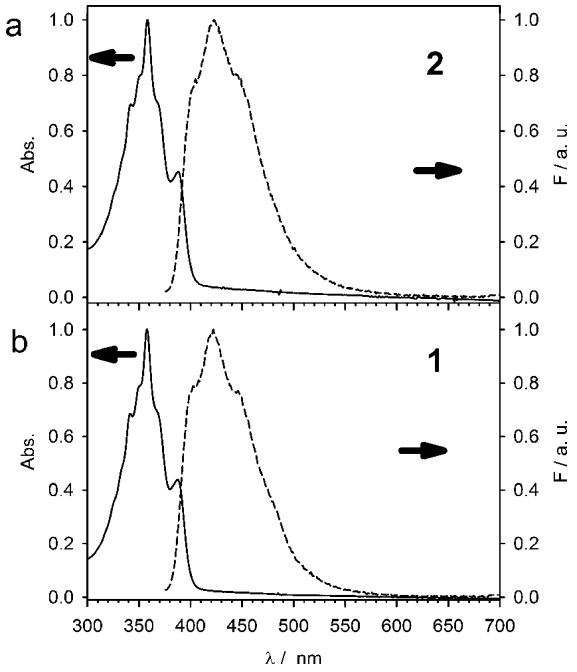

Figure 1. Normalized absorption (left axis) and emission (right axis) spectra for compounds **1** and **2** (10 μM) in $CHCl_3$. λ_{ex} = 357 nm: (a) compound **1**, (b) compound **2**.

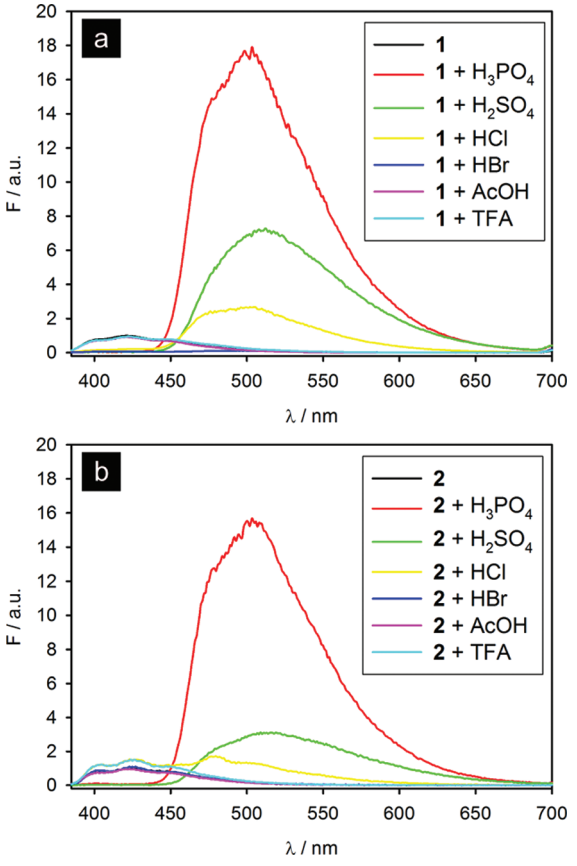

Figure 2. Emission spectra of compounds **1** and **2** (10 μM) after addition of 25 equiv of each acid in $CHCl_3$. λ_{ex} = 357 nm: (a) compound **1**, (b) compound **2**.

According to the expected acid–base properties of the compounds involved, the interaction of the triprotonated receptor with $H_2PO_4^-$ can be considered in highly acidic media. Thus, the origin of the recognition of H_3PO_4 by **1** and **2** could rely on the protonation of the receptor and the stabilization of the triprotonated species by the $H_2PO_4^-$ anion, which is not accomplished with HSO_4^- or the other anions assayed. This process would involve the protonation of the basic nitrogen atom of the acridine moiety, leading to a strongly fluorescent acridinium substructure.[68]

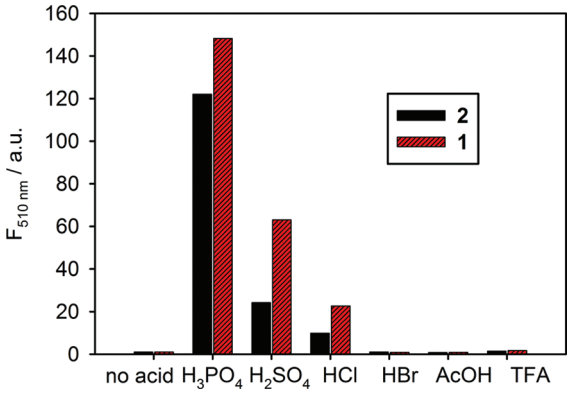

Figure 3. Normalized fluorescence intensity at 510 nm of compounds **1** and **2** (10 μM) upon addition of 25 equiv of each acid in $CHCl_3$. λ_{ex} = 357 nm.

The participation of a complex species involving the protonated receptor interacting with $H_2PO_4^-$ was confirmed by the following experiments. First, no change in fluorescence was observed when compound **1** or **2** were titrated with tetrabutylammonium dihydrogen phosphate ($TBAH_2PO_4$). Similarly, the addition of an excess of a strong acid such as TFA did not produce significant changes in the fluorescence, therefore the enhanced fluorescence cannot be only due to a protonation event but to a combined effect of proton and anion. To corroborate this 50 equivalents of TFA were added to receptors **1** and **2** followed by a titration with $TBAH_2PO_4$. As can be seen in Figure 4, this led to an increase in fluorescence.

In order to fully characterize the photophysical and acid–base properties of compounds **1** and **2**, fluorescence measurements in water were carried out. To better understand the results obtained from these studies, the corresponding photophysical parameters describing the fluorescence of compounds **1** and **2** in this solvent were initially determined with the use of both steady-state and time-resolved fluorescence (time correlated single photon counting technique, TCSPC) measurements. The fluorescence parameters for the parent acridine were also determined for comparison. The results obtained are shown in Table 1. Variations in the pH of the solutions were achieved by adding small aliquots of H_2SO_4 or NaOH. The samples were purged with nitrogen before any measurement.

Values of quantum yield and fluorescence lifetime obtained for acridine at acid and basic pH correspond with those reported in the literature.[69−73] The quantum yields obtained for **1** and **2** at acidic pH were very similar (0.43 and 0.38 respectively) and slightly lower than those calculated for acridine itself (0.65). The quantum yield seems to undergo an important decrease upon basification of the medium, although the low solubility of the pseudopeptidic receptors only allowed carrying out the measurement in a small pH range. Values for the different fluorescence (τ_F) lifetimes were obtained by

dx.doi.org/10.1021/jo202077v | J. Org. Chem. 2012, 77, 490–500

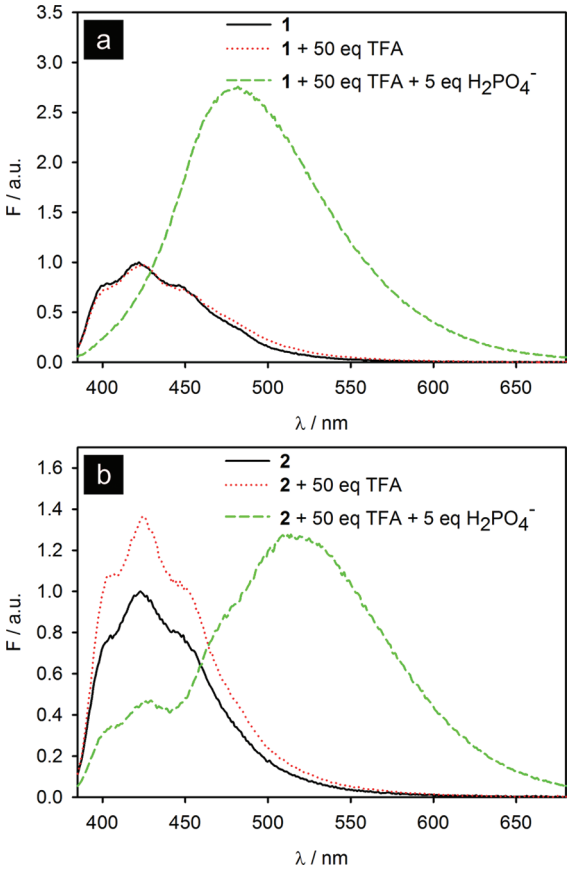

Figure 4. Fluorescence emission in $CHCl_3$ of **1** and **2** (10 μM) without and with TFA in the presence of $TBAH_2PO_4$. λ_{ex} = 357 nm: (a) compound **1**, (b) compound **2**.

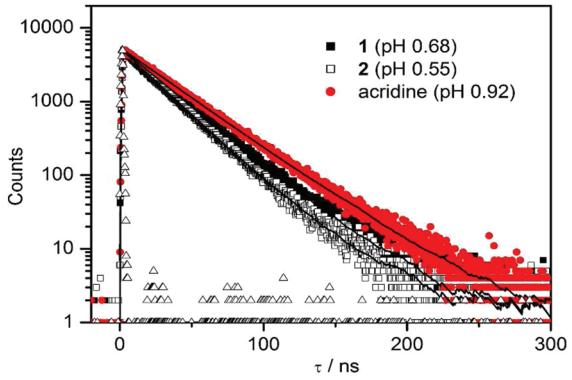

Figure 5. Fluorescence decay curves of compounds **1**, **2**, and acridine (20 μM in water, pH adjusted with H_2SO_4) in acidic aqueous solution (λ_{exc} = 372 nm/ λ_{em} = 475 nm). The incident light pulse is also shown (open triangles).

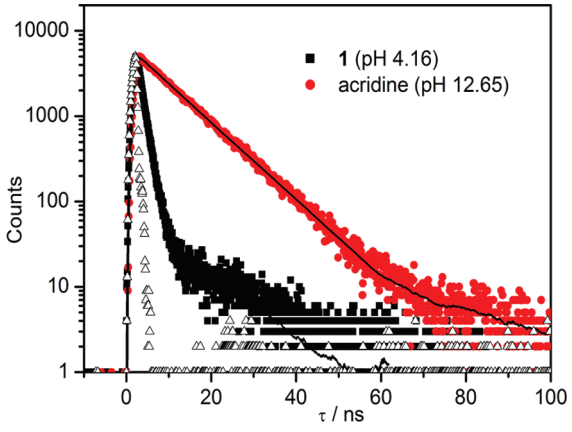

Figure 6. Fluorescence decay curves of compounds **1** and acridine (20 μM in water, pH adjusted with NaOH and H_2SO_4) in less acidic aqueous solution (λ_{exc} = 372 nm/ λ_{em} = 426 nm). The incident light pulse is also shown (open triangles).

deconvolution of the experimental curves (Figures 5 and 6). The lifetime values determined for the pseudopeptidic receptor **1** were smaller than those for the parent acridine. In the case of compound **1** at pH = 4.16 the experimental curve indicated the participation of a second lifetime, being the contribution of the shorter lifetime much higher than the contribution of the longer lifetime.

The variation in the fluorescence of the receptors upon modification of the pH was used to determine the corresponding pK_a values for the protonation of the acridine moiety. Figure 7 shows the main differences in the fluorescence spectra for **1** and **2** at two different pH values and the resulting titration curves are shown in Figure 8. The pK_a values obtained for compounds **1** and **2**, and shown in Table 1, revealed some interesting trends. The pK_a of the third protonation of the macrocyclic compound **2** (pK_a ~ 1.7), which leads to the formation of strongly fluorescent acridinium species, is lower than that of the open chain compound **1** (pK_a ~ 2.7). This trend can be explained by taking into account that in macrocycle **2** the two initial ammonium groups are closer to the third protonated site due to the rigidity of the macrocyle. In contrast, in the case of the open-chain compound **1**, its higher conformational flexibility can allow to adopt conformations in which the two ammonium groups are located as far as possible from the acridinium unit to minimize the electrostatic repulsion. Therefore, it is more difficult to protonate the acridine unit in the macrocyclic compound **2** justifying the difference of 1 order of magnitude in the acidities. Nevertheless, once the

Table 1. Fluorescence Properties for Compounds 1 and 2 in Water (Measurements Made with a Compound Concentration of 20 μM in Water Using H_2SO_4 and NaOH To Adjust the pH)

	pH	λ_{abs} (nm)	λ_{exc} (nm)	λ_{em} [d] (nm)	ES_1 (kcal/mol)	Φ_F [e]	τ_1 [f] (ns)	α_1 (%)	τ_2 [f] (ns)	α_2 (%)	χ^2	pK_a
acridine	0.92	354, 398	354[a]	477	65.9	0.65	31.6[g]				1.03	5.42[i]
	12.65	355	354[b]	427	72.7	0.24	9.5[h]				1.22	
2[j]	0.55	359, 397	359[a]	502	62.7	0.38	23.9[g]				1.15	1.67 ± 0.02
1	0.68	358, 398	359[a]	501	62.6	0.43	26.6[g]				1.15	2.74 ± 0.01
	4.16	357	356[c]	432	71.8	0.05	1.3[h]	95.43	12.2[h]	4.57	0.96	

[a] λ_{em} = 540 nm. [b] λ_{em} = 470 nm. [c] λ_{em} = 450 nm. [d] λ_{exc} = 366 nm. [e] Quinine sulfate standard (aqueous H_2SO_4 0.1 M, air). Φ_F = 0.53 (taken from ref 73). [f] λ_{exc} = 372 nm. [g] λ_{em} = 475 nm. [h] λ_{em} = 426 nm. [i] Taken from ref 69. [j] It was not possible to measure this sample at pH 4 due to precipitation of the product.

dx.doi.org/10.1021/jo202077v | J. Org. Chem. 2012, 77, 490–500

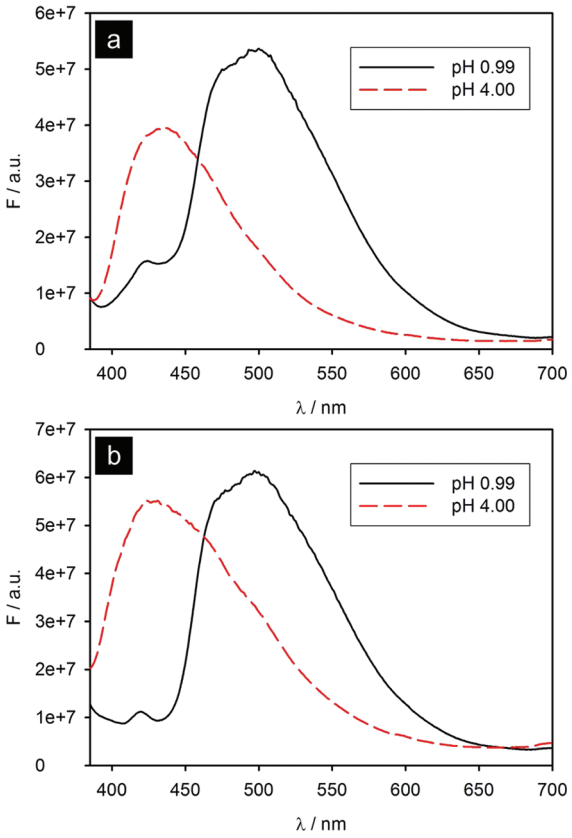

Figure 7. Fluorescence spectra at different pH: (a) compound **1**, λ_{ex} = 366 nm; (b) compound **2**, λ_{ex} = 368 nm. Probe concentration: 10 μM in aqueous solution (1% DMSO).

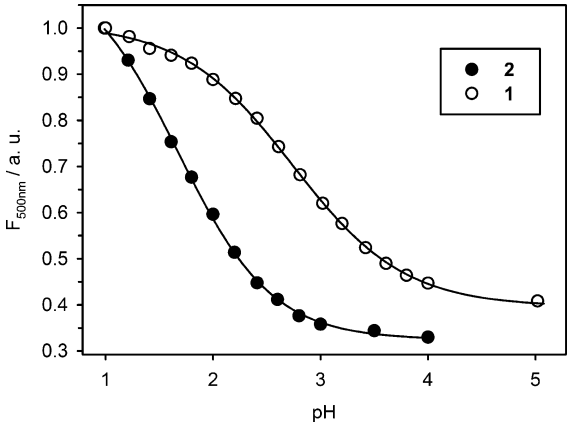

Figure 8. Fluorescence pH titration of compounds **1** and **2**, monitoring emission at 500 nm. Probe concentration: 10 μM in aqueous solution (1% DMSO). λ_{ex} = 368 nm for **2** and λ_{ex} = 366 nm for **1**. For compound **1** pK_a = 2.74 ± 0.01; for compound **2** pK_a = 1.67 ± 0.02.

acridine nitrogen atom is protonated, the photophysical behavior is quite similar.

As can be deduced from Table 1 the behavior of compounds **1** and **2** in acidic medium is comparable to the one displayed by acridine; i.e., the emitting species at long wavelength is clearly the acridinium cation which displays fluorescence (ES_1 ~ 62–66 kcal/mol and τ_1 ~ 24–32 ns) properties clearly different to those of the parent acridine (ES_1 ~ 72 kcal/mol and τ_1 < 10 ns). Hence, from these data in aqueous medium we can conclude that the fluorescent moiety in the supramolecular complex formed between **1** or **2**, and $H_2PO_4^-$ or HSO_4^- in $CHCl_3$ is always the acridinium fluorophore.

The overall protonation scheme for the open-chain compound **1** and macrocycle **2** must consider three steps as shown in Figure 9 for receptor **2**. First, protonation of the

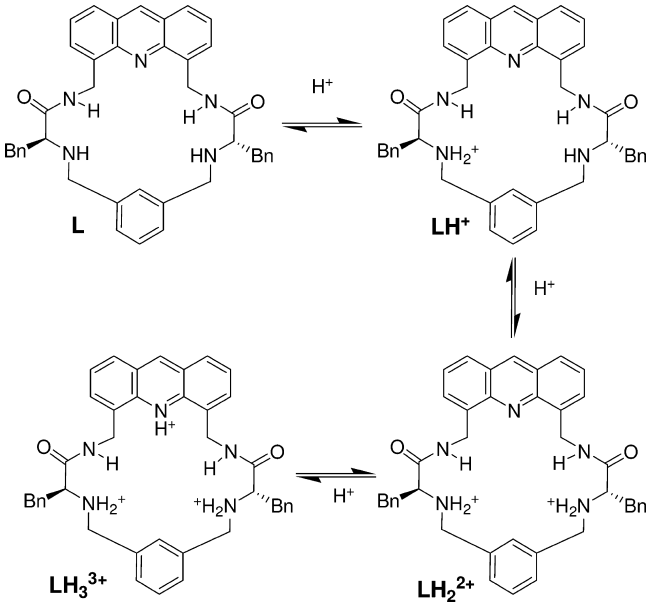

Figure 9. Overall protonation scheme for the macrocycle **2**.

amines takes place, followed by that of the acridine unit, accordingly to the bigger basicity of the secondary amines as compared to the acridine. The isosbestic point observed in the titrations confirms that the observed fluorescence change is due to the equilibrium between the diprotonated (LH_2^{2+}) and triprotonated (LH_3^{3+}) species; see the Supporting Information. A similar protonation scheme can be drawn for the open-chain compound **1**. It must be pointed out that solvent has an important effect on the recognition process. In water the solvation energy is larger than the host–guest binding energy. Thus, spectra from titrations in water show an isosbestic point due to equilibrium observed between the triprotonated and the diprotonated receptor and no supramolecular species are detected. In contrast, in chloroform, solvation energy is not as important and supramolecular interactions play an important role. In this case, the spectra obtained from titrations did not show an isosbestic point indicating the participation of different species in the recognition process.

^{1}H NMR Spectroscopic Experiments. NMR experiments were also carried out in order to confirm the suggested protonation sequence. NMR titration experiments of compound **2** showed that the addition of 2 equiv of TFA protonates the two secondary amines. The protonation of the acridine, as indicated by a downfield shift of ca. 1 ppm for the acridine signal at 8.75 ppm, is more difficult. As shown in Figure 10, a large concentration of TFA (350 mM), much above 3 equiv, has to be added to protonate the acridine in compound **2** (Figure 10c).

Titration of compound **1** could not be carried out due to precipitation of the product. Nevertheless, the triprotonated compound **1** is soluble in $CHCl_3$, and the ^{1}H NMR spectrum could be recorded (Figure 11). It can be seen that in triprotonated compound **1** the acridine CH_2 protons are non

dx.doi.org/10.1021/jo202077v | J. Org. Chem. 2012, 77, 490–500

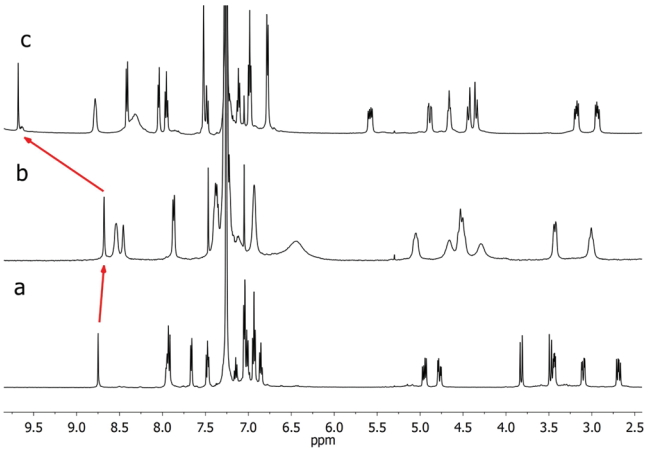

Figure 10. ^{1}H NMR titration of **2** in $CDCl_3$ in the presence of different concentration of TFA. Probe concentration, 5 mM: (a) TFA 0 mM, (b) TFA 10 mM (2 equiv) (a precipitate was formed), (c) TFA 350 mM (all the precipitate was redissolved). Arrows show the variation of the 9H of the acridine moiety in compound **2**.

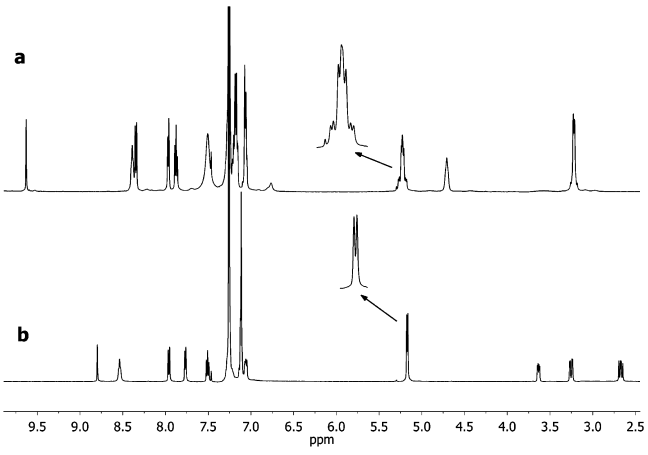

Figure 11. ^{1}H NMR titration of **1** in $CDCl_3$ with TFA. Probe concentration, 5 mM: (a) TFA, 0 mM; (b) TFA, 350 mM. An expansion of the signals corresponding to the acridine-CH_2 protons of each trace is given.

equivalent (see expansions in Figure 11) suggesting that for this protonation state the conformation is more rigid.

Computational Calculations. In order to investigate the potential interaction of anions $H_2PO_4^-$ and HSO_4^- with triprotonated **1** and **2** species, computational studies were performed. To reduce computational cost, the benzene ring of the amino acid side chain in structures **1** and **2** was replaced by an H atom, yielding structures **6** and **7**, respectively (see the Supporting Information). First, the minimum conformers of the L, LH^+, LH_2^{2+}, and LH_3^{3+} species (with L being **6** and **7**) were located performing a Monte Carlo conformational search with Spartan '08 at the MMFF level of theory. The same calculation was then performed for the complexes $H_2PO_4^-\cdot LH_3^{3+}$ and $HSO_4^-\cdot LH_3^{3+}$. The resulting geometries were minimized with Gaussian 03 at the B3LYP/6-31G* level of theory. Computational models (Figure 12) show that the anions $H_2PO_4^-$ and HSO_4^- interact with the triprotonated receptor with the participation of an H-bond between the H of the acridinium fragment and the anion. The calculated Gibbs free energies for the interaction are −219.46 kcal/mol for

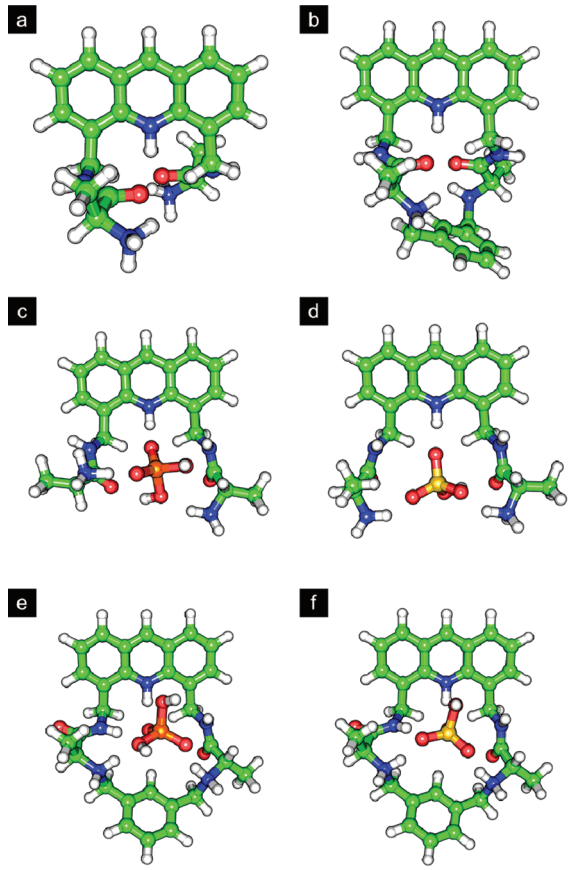

Figure 12. Optimized geometries at the B3LYP/6-31G* level of theory: (a) $\mathbf{6}H_3^{3+}$, (b) $\mathbf{7}H_3^{3+}$, (c) $H_2PO_4^-\cdot\mathbf{6}H_3^{3+}$, (d) $HSO_4^-\cdot\mathbf{6}H_3^{3+}$, (e) $H_2PO_4^-\cdot\mathbf{7}H_3^{3+}$, (f) $HSO_4^-\cdot\mathbf{7}H_3^{3+}$.

$H_2PO_4^-\cdot\mathbf{6}H_3^{3+}$, −209.40 kcal/mol for $HSO_4^-\cdot\mathbf{6}H_3^{3+}$, −215.74 kcal/mol for $H_2PO_4^-\cdot\mathbf{7}H_3^{3+}$, and −203.85 kcal/mol for $HSO_4^-\cdot\mathbf{7}H_3^{3+}$. Therefore, those results suggest that for compound **1** the binding energy of its triprotonated form with $H_2PO_4^-$ can be 10.07 kcal/mol more favorable than that for HSO_4^-, while for compound **2** the difference is slightly higher (11.89 kcal/mol more favorable). These computational results are in good agreement with the experimental fluorescence studies in $CHCl_3$ and can be used to rationalize the observed selectivity.

A hydrogen bonding analysis of the structures of the different supramolecular complexes formed between triprotonated **6** and triprotonated **7** with the different anions is also useful for a better understanding of the stabilities found.[74] For this purpose, a Monte Carlo conformational search with the MMFF force field, as implemented in Spartan'08, was carried out for each protonated species in order to have a wide range of conformers. The most stable conformer for each species was fully optimized at the B3LYP/6-31G* level of theory with the Gaussian 03 software, and then the H-bond distances were measured (see Supporting Information). It can be observed that the open chain compound **6** and its protonated species, and accordingly the related receptor **1**, are able to form a higher number of intramolecular hydrogen bonds than the macrocyclic compound **7** and its protonated derivatives (see the Supporting Information). Considering the last protonation step, it can be observed that the diprotonated open-chain compound **6** is predicted to form two hydrogen bonds while the triprotonated **6** can form four hydrogen bonds. In contrast, for macrocycle

dx.doi.org/10.1021/jo202077v | J. Org. Chem. 2012, 77, 490−500

7 both the monoprotonated and the triprotonated species can form three hydrogen bonds (see Table 2). Therefore, the

Table 2. Hydrogen Bonds[a] Found in the Optimized Geometries for Reactants and Products at the Different Protonation Steps for 6 and 7

	6		7	
reaction	reactants	products	reactants	products
H + L = HL	6	5	2	3
H + HL = H_2L	5	2	3	3
H + H_2L = H_3L	2	4	3	3

[a]Number of hydrogen bonds detected as defined by a H···X distance < 2.65 Å.

potential stabilization of the $\mathbf{6}H_3^{3+}$ species through the presence of those two additional hydrogen bonds after protonation of $\mathbf{6}H_2^{2+}$ supports the difference of the pK_a observed experimentally between **1** and **2**.

The same analysis can be carried out to rationalize the stability of the complexes formed. Considering the formation of $\mathbf{L}H_3^{3+}X^-$ species, we must bear in mind that for compound $\mathbf{6}H_3^{3+}$ four hydrogen bonds are formed, whereas in macrocyclic compound $\mathbf{7}H_3^{3+}$ (due to conformational restrains conferred by the macrocyclic geometry) only three hydrogen bonds can be formed. In the calculated structure for the complex $H_2PO_4^-\cdot\mathbf{6}H_3^{3+}$ there are five intermolecular hydrogen bonds between the $H_2PO_4^-$ anion and $\mathbf{6}H_3^{3+}$, as well as one intramolecular hydrogen bond. In the structure for the complex $HSO_4^-\cdot\mathbf{6}H_3^{3+}$ there are four hydrogen bonds between the HSO_4^- anion and $\mathbf{6}H_3^{3+}$ and two intramolecular hydrogen bonds. These data clearly support the selective recognition of $H_2PO_4^-$ in the presence of HSO_4^-. Besides, energy calculations for both complexes indicate an energy difference of about 10 kcal/mol in favor of the complex with $H_2PO_4^-$. In the optimized structure for the complexes $H_2PO_4^-\cdot\mathbf{7}H_3^{3+}$ and $HSO_4^-\cdot\mathbf{7}H_3^{3+}$ there are five hydrogen bonds between the anion and the triprotonated ligand, and no intramolecular hydrogen bonds are observed. On the other hand, it must be noted that for all five hydrogen bonds the anion is acting as the hydrogen acceptor, the hydrogen atoms of the anions being located at the outer surface of the complex. Thus, the atoms bearing the negative charge are located much closer to the cationic ammonium groups. The situation is different to that found for the complexes formed by $\mathbf{6}H_3^{3+}$ for which the anions act both as hydrogen donors and acceptors. Thus, the calculated structures for the complexes from $\mathbf{7}H_3^{3+}$ suggest that the preorganization of the macrocyclic structure provides an excellent complementarity between this triprotonated receptor and $H_2PO_4^-$ or HSO_4^- anions, leading to an optimization of electrostatic interactions and hydrogen bonding. Again, energy calculations reveal a higher stability (ca. 10 kcal/mol) for the complex with the $H_2PO_4^-$ anion.

X-ray Studies. Single crystals of $[\mathbf{2}\text{-}H_2](H_2PO_4)_2$ suitable for X-ray diffraction were grown from the slow evaporation of a solution of **2** with 10 equiv of H_3PO_4 in a water, methanol and acetonitrile mixture (Figure 13). Under these conditions, the acridine unit of compound **2** should not be protonated. This is consistent with the protonation patterns for the acridine unit detected with the other techniques used.

The solid-state structure[75] shows the macrocycle to have adopted an essentially self-filling conformation stabilized by an intramolecular $\pi-\pi$ interaction between the acridine unit and

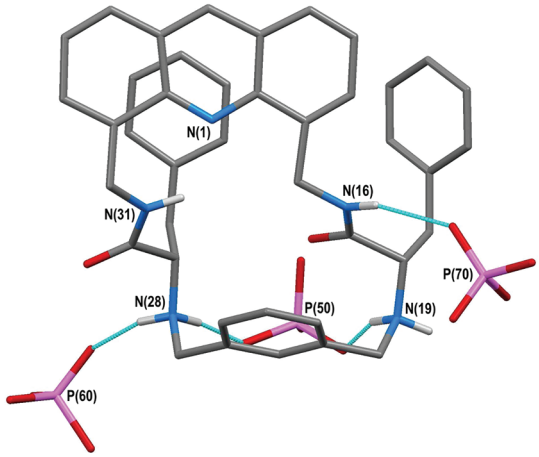

Figure 13. Molecular structure of a crystal of $[\mathbf{2}\text{-}H_2](H_2PO_4)_2$ highlighting the presence of the phosphate groups.

one of the terminal phenyl rings (with centroid···centroid and mean interplanar separations of ca. 3.91 and 3.60 Å, respectively). The two amide groups have markedly different orientations with respect to the nitrogen of the acridine moiety, the N(16)- and N(31)-based amides adopting *anti* and *syn* conformations respectively. The latter allows for an intramolecular N−H···N hydrogen bond [N(31)···N(1) 2.873(12) Å], though the location of the hydrogen atom could not be determined; modeled as being located on N(31) with an N−H distance of 0.90 Å, the H···N separation and N−H···N angle are 2.24 Å and 127°, respectively). This intramolecular N···N contact precludes the protonation of both nitrogens involved as this would result in an H···H separation of ca. 1.52 Å. The conformation of the macrocycle also places the N(16)-based amide unit proximal to the 1,3-xylenyl ring with a C···C separation between the amide carbon and the proximal substituted carbon of the aryl ring of ca. 2.98 Å.

The PO_4 units (whose protonation could not be unambiguously determined) sit outside the macrocycle, but on account of the disorder in the structure[75] only the heteroatom separations are worth considering. The N(16) amide nitrogen is approached by the oxygen of the 50% occupancy O(81)-based water molecule at ca. 2.74 Å, and alternatively by one of the oxygen atoms of the 50% occupancy P(70)-based H_3PO_4 unit at ca. 3.20 Å. The N(19) amine nitrogen is linked to an oxygen of the P(50)-based $H_2PO_4^-$ anion at ca. 2.76 Å and to an oxygen of the major occupancy orientation of the P(60)-based $H_2PO_4^-$ anion at ca. 2.82 Å. Similarly, the N(28) amine nitrogen is linked to an oxygen of the P(50)-based $H_2PO_4^-$ anion at ca. 2.71 Å and to an oxygen of the major occupancy orientation of the P(60)-based H_2PO_4 anion at ca. 2.74 Å.

As indicated above, from the X-ray crystal structure it was not possible to unambiguously locate the protons on the amines or acridine group. Therefore, fluorescence experiments in the solid state were also carried out by putting a few crystals in a glass surface. The results obtained are displayed in Figure 14 and Table 3. Both the qualitative and quantitative analysis of the spectra reveal an excellent agreement with those corresponding to a 20 μM solution of **2** at pH = 4. According to previous experiments, this pH value corresponds to a region for which the nitrogen atom of the acridine moiety is not protonated.

dx.doi.org/10.1021/jo202077v | J. Org. Chem. 2012, 77, 490−500

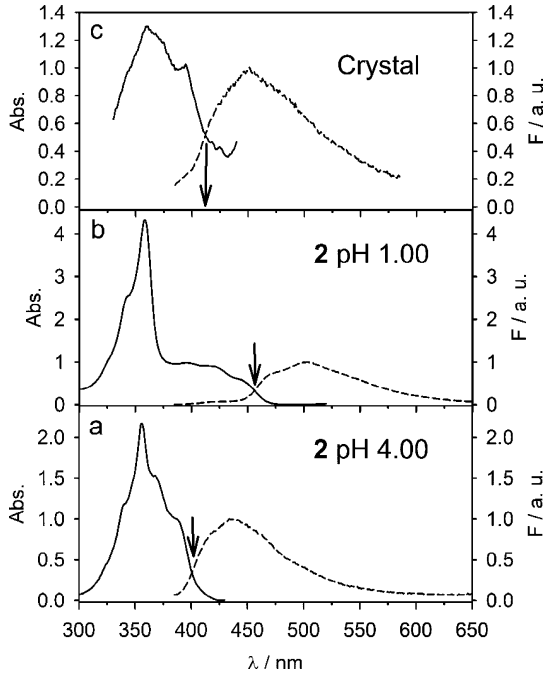

Figure 14. Normalized excitation and emission spectra for macrocycle **2** in a concentration 20 μM (water, 2% DMSO, and pH adjusted with $HClO_4$, and NaOH) at (a) pH 4.00, (b) pH 1.00, and (c) for the crystals obtained from compound **2** and 10 equiv of phosphoric acid.

Table 3. Fluorescence Measurements 20 μM in Water (2% of DMSO) and pH Adjusted with NaOH/$HClO_4$

	$E(S_1) - E(S_0)$ (kcal/mol)
acridine pH 1.00	65.9
acridine pH 9.84	72.5
2 pH 1.00	62.7
2 pH 4.00	71.4
1 pH 1.00	62.8
1 pH 4.00	71.7
crystal $2H_2^{2+}{\cdot}2H_2PO_4^-$	67.6

In order to rationalize and confirm these results, computational studies for the model compound 4,5-dimethylacridine were carried out in the gas phase at the B3LYP/6-31G* level of theory using the Gaussian 09 software. The geometry of the 4,5-dimethylacridine molecule interacting with one proton was optimized for several N···H distances at the fundamental and first excited state. The S_1-S_0 energy gap was then obtained as the difference in energy of the optimized structures for the fundamental and first exited state. A final reference structure was optimized for 4,5-dimethylacridine considering the proton at an infinite distance (see Figure 15).

From these calculations, we can conclude that the interaction of the N of the acridine unit with one proton has a big effect on the S_1-S_0 energy gap. As can be seen in Figure 15 the experimental energy gap (67.6 kcal/mol) corresponds to the presence of a large N(acridine)···H distance, which is more appropriate for an acridine nitrogen acting as a hydrogen bond acceptor than for an acridinium group acting as a hydrogen bond donor.

CONCLUSIONS

We have designed, synthesized, and characterized two pseudopeptidic receptors for the efficient and selective complexation

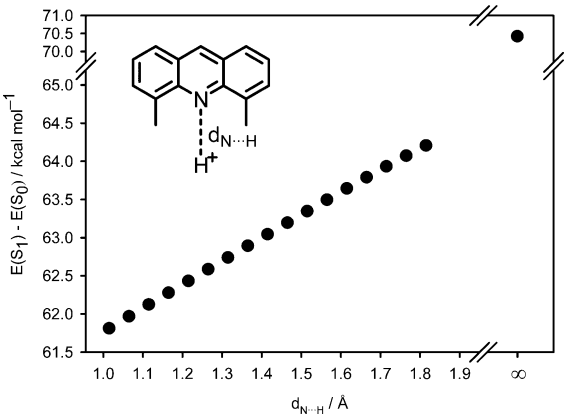

Figure 15. S_1-S_0 energy difference for the fundamental and first exited state of model compound 4,5-dimethylacridine interacting with a proton at different N···H distances.

of $H_2PO_4^-$ in chloroform in acidic media. Macrocyclic compound **2** was found to be more selective toward $H_2PO_4^-$ than the open-chain compound **1** versus other anions such as HSO_4^-, acetate, trifluoroacete, chloride, and bromide. Under these conditions, a selective detection of $H_2PO_4^-$ can be accomplished through fluorescence signaling. The process has been studied in detail both experimentally and with the help of high level calculations at the B3LYP/6-31G* level. The whole set of data reveal that both ligands (**1** and **2**) show, when triprotonated, a high level of complementarity to the $H_2PO_4^-$ anion, being able to provide a stronger interaction than that for HSO_4^- or other anions. The differences observed between **1** and **2** must be associated to the higher level of preorganization of the macrocyclic structure of **2**. It has been demonstrated that the observed fluorescence in the presence of the guest is associated to the conversion of the acridine moiety of the receptor into a strongly emitting acridinium fluorophore.

EXPERIMENTAL SECTION

Materials and Methods. All commercially available reagents and solvents were used as received, without further purification. Acridine was recrystallized from an ethanol–water mixture as described previously.[70]

Steady-State Fluorescence Spectroscopy. For fluorescence titrations in water, steady-state fluorescence spectra were recorded in a fluorimeter equipped with a 450 W xenon lamp. Fluorescence spectra were recorded in the front face mode. For fluorescence titrations in chloroform the emission spectra were recorded between 367 and 700 nm with an excitation wavelength of 357 nm.

Time-Resolved Fluorescence Spectroscopy. Time-resolved fluorescence measurements were done with the technique of time correlated single photon counting (TCSPC). Samples were excited with an IBH 372 nm NanoLED with a fwhm of 1.3 ns and a repetition rate of 100 kHz. Data were fitted to the appropriate exponential model after deconvolution of the instrument response function by an iterative deconvolution technique, using the IBH DAS6 fluorescence decay analysis software, where reduced χ^2 and weighted residuals serve as parameters for goodness of fit.

Nuclear Magnetic Resonance. ^1H and ^{13}C NMR spectra were recorded on a 500 MHz spectrometer (500 MHz for ^1H and 125 MHz for ^{13}C) or a 300 MHz spectrometer (300 MHz for ^1H and 75 MHz for ^{13}C).

Fluorescence Measurements. *pH Titrations in Chloroform.* Compounds were dissolved in $CHCl_3$ to obtain 10 mM stock solutions, then were diluted to 10 μM. These solutions were titrated by adding increasing volumes of stock solutions of the acids of 0.005–0.05 M in $CHCl_3$ with a 2% of methanol.

dx.doi.org/10.1021/jo202077v | J. Org. Chem. 2012, 77, 490–500

pH Titrations in Water. Compounds were dissolved in dimethyl sulfoxide (DMSO) to obtain 1 mM stock solutions and then were diluted to 10 μM with water containing a mixture of several buffers to facilitate titrations between pH 9 and 1 (40 mM of each sodium salt: acetate, phosphate, borate, and carbonate). The small percentage of DMSO (1−2%) was required to avoid the precipitation of the compounds due to low solubility in water. Slight variations in the pH of the solutions were achieved by adding the minimum volumes of 0.1−1.0 M NaOH or 0.1−1.0 M HCl (typically 10 μL added to 10 mL), in such a way that dilution effects were negligible.[76] pK_a values where obtained from the nonlinear curve-fitting of the data with Origin 6.1.

Fluorescence Lifetime Determination. Compounds were dissolved in water and H_2SO_4 to obtain stock solutions (1 mM), and then they were diluted to 20 μM with water. Variations in the pH of the solutions were achieved by adding H_2SO_4 or NaOH. Samples were purged with nitrogen.

Quantum Yield Determination. Solutions of the compounds were prepared as described for the fluorescence lifetime determination. Fluorescence quantum yields of compounds **1**, **2**, and acridine are reported relative to quinine sulfate (aqueous solution H_2SO_4 0.1 M, air); Φ_F = 0.53. The experiments were done using optically matching solutions. Emission spectra was recorded upon excitation at λ_{exc} = 366 nm. The quantum yield was calculated using eq 1. In this expression, it is assumed that the sample and the reference are excited at the same wavelength so that it is not necessary to correct for the different excitation intensities of different wavelengths.

$$\Phi_f = \Phi_r \times (A_r F_s / A_s F_r) \times (n_s^2 / n_r^2) \quad (1)$$

Here, Φ_f is the quantum yield, F is the integrated intensity, A is the optical density, and n is the refractive index. The subscript r refers to the reference fluorophore of known quantum yield and subscript s to the sample.

Computational Studies. Monte Carlo conformational searches at MMFF force field were carried out with the Spartan '08 software.[77] Calculations of model compounds **5** and **6**, and their supramolecular complexes were performed at the B3LYP/6-31G* level of theory using the Gaussian 03 software.[78] All geometries were fully optimized and it was checked to be true minima by the analysis of the vibration normal modes. Calculations for the interaction of 4,5-dimethylacridine with a proton were carried out in the gas phase at the B3LYP/6-31G* level of theory using the Gaussian 09 software.[79] No symmetry constraints were used. First excited state optimizations were performed using the TD = (NStates = 6, Root = 1) parameters.

Experimental Procedures. *Synthesis of Compound* ***5***. 4,5-Bis(aminomethyl)acridine·2HCl (0.200 g, 0.645 mmol) was placed in a 50 mL round-bottom flask, and 1 M aqueous NaOH (10 mL) and MeOH (1 mL) were added. After complete dissolution of the solid, the solution was extracted three times with dichloromethane (15 mL). The organic layers were collected and dried with anhydrous $MgSO_4$. The solvent was then vacuum evaporated to afford 4,5-bis-(aminomethyl)acridine (0.142 g, 0.600 mmol, yield 93%) as a yellowish solid. This was dissolved in DME (15 mL) in a 50 mL round-bottom flask. Cbz-L-Phe-OSuc (**4**) (0.476 g, 1.20 mmol) was dissolved in DME (10 mL) and slowly added to the reaction flask. A white precipitate was rapidly formed, and the mixture was stirred at room temperature for 8 h and then at 50 °C for 5 h. After cooling, the white precipitate was filtered and washed with cold water (50 mL) and a small amount of methanol to afford the expected compound **5** as a white solid (0.443 g, 5.55 mmol, 85% yield): mp 260−263 °C; $[\alpha]^{25}_D$ = +34.12 (*c* 0.01, DMSO); IR (ATR) 3284, 1649, 1454 cm^{-1}; ^{1}H NMR (500 MHz, DMSO-d_6) δ 9.10 (s, 1H), 8.57 (t, 2H, *J* = 5.3 Hz), 8.00−8.10 (m, 2H, m), 7.60 (d, 2H, *J* = 8.4 Hz), 7.52 (d, 4H, *J* = 4.9 Hz), 7.09−7.36 (m, 20H), 5.09 (m, 4H), 4.93 (q, 4H, *J* = 12.7 Hz), 4.41 (dd, 2H, *J* = 9.0, 13.7 Hz), 3.07 (dd, 2H, *J* = 4.6, 13.5 Hz), 2.85 (dd, 2H, *J* = 10.4, 13.1 Hz); ^{13}C NMR (75 MHz, DMSO-d_6) δ 172.3, 156.6, 146.2, 138.7, 137.7, 137.3, 137.2, 129.9, 128.9, 128.7, 128.3, 128.1, 128.0, 127.8, 126.9, 126.6, 126.3, 66.0, 57.2, 39.4, 38.3; HRMS (ESI-TOF)$^+$calcd for $C_{49}H_{45}N_5O_6$ (M + H)$^+$ 800.3448, found 800.3463. Anal. Calcd for $C_{49}H_{45}N_5O_6$: C, 73.57; H, 5.67; N, 8.76. Found: C, 73.43; H, 5.82; N, 8.75.

Synthesis of Compound ***1***. Compound **5** (2.167 g, 2.71 mmol) was placed into a 100 mL round-bottom flask, and then a 33% HBr/AcOH solution (50 mL) was added. After complete dissolution of the solid, a yellow solution was formed. The reaction was stirred under a nitrogen atmosphere for 1 h. The resulting colorless solution was poured into a 250 mL beaker containing diethyl ether (150 mL). A white precipitate was formed and was filtered and the solid washed with ether. The solid was redissolved in distilled water (30 mL), and the solution was washed twice with $CHCl_3$ (30 mL) and, finally, was basified with solid NaOH until pH 12−13. NaCl was added until saturation, and the aqueous phase was extracted three times with $CHCl_3$ (30 mL). The organic phase was dried with anhydrous $MgSO_4$, and the solvent was vacuum eliminated to afford compound **1** as a white solid (1.297 g, 2.439 mmol, 90% yield): mp 83−85 °C; $[\alpha]^{25}_D$ = −47.98 (*c* 0.01, DMSO); IR (ATR) 3288, 1648, 1430 cm^{-1}; ^{1}H NMR (500 MHz, $CDCl_3$) δ 8.70 (s, 1H), 8.45 (t, 2H, *J* = 5.4 Hz), 7.87 (d, 2H, *J* = 8.5 Hz), 7.69 (d, 2H, *J* = 6.7 Hz), 7.43 (t, 2H, *J* = 7.6 Hz), 7.03−7.10 (m, 7H, m), 6.92−7.03 (m, 2H), 5.10 (d, 4H, *J* = 6.1 Hz), 3.58 (dd, 2H, *J* = 3.9, 8.8 Hz), 3.19 (dd, 2H, *J* = 4.0, 13.7 Hz), 2.62 (dd, 2H, *J* = 9.1, 13.6 Hz), 1.40 (s, 4H); ^{13}C NMR (126 MHz, $CDCl_3$) δ 174.0, 146.7, 137.9, 136.7, 136.1, 129.5, 129.1, 128.3, 127.7, 126.6, 126.4, 125.7, 56.7, 41.1, 40.7; HRMS (ESI-TOF)$^+$calcd for $C_{33}H_{33}N_5O_2$ (M + H)$^+$ 532.2713, found 532.2717. Anal. Calcd for $C_{33}H_{33}N_5O_2$: C, 74.55; H, 6.26; N, 13.17. Found: C, 74.38; H, 6.37; N, 13.00.

Synthesis of Compound ***2***. Compound **1** (0.500 g, 0.941 mmol), TBABr (0.1516 g, 0.470 mmol), and DiPEA (1.611 mL, 9.41 mmol) were placed in a 250 mL round-bottom flask, and then dry acetonitrile (134 mL) was added. The reaction mixture was stirred at room temperature until complete dissolution of the reagents, and then α, α'-dibromo-*m*-xylene (0.248 g, 0.941 mmol) dissolved into a small amount of dry acetonitrile was added. The reaction was maintained heated by a temperature gradient from 50.0 to 81.6 °C (reflux) for 24 h, under a nitrogen atmosphere. After cooling, the solvent was vacuum eliminated. Purification of the crude was carried out by column chromatography over flash silica gel (dichloromethane/methanol from 100:0 to 100:5 with a few drops of aqueous ammonia added). The macrocycle was obtained as a white solid (0.507 g, 0.800 mmol, 85% yield): mp 89−90 °C; $[\alpha]^{25}_D$ = +41.44 (*c* 0.01, $CHCl_3$); IR (ATR) 3317, 2919, 1653, 1430; ^{1}H NMR(500 MHz, $CDCl_3$) δ 8.73 (s, 1H), 7.85−8.00 (m, 4H), 7.66 (d, 2H, *J* = 6.7 Hz), 7.47 (dd, 2H, *J* = 6.9, 8.3 Hz), 7.25 (s, 1H), 7.13 (d, 1H, *J* = 7.6 Hz), 7.04 (d, 4H, *J* = 7.3 Hz), 7.01 (dd, 2H, *J* = 1.3, 7.6 Hz), 6.93 (t, 4H, *J* = 7.6 Hz), 6.86 (d, 2H, *J* = 7.4 Hz), 4.95 (dd, 2H, *J* = 7.5, 14.9 Hz), 4.79 (d, 2H, *J* = 5.7 Hz), 3.82 (d, 2H, *J* = 12.8 Hz), 3.49 (d, 2H, *J* = 12.8 Hz), 3.44 (dd, 2H, *J* = 4.7, 8.6 Hz), 3.10 (dd, 2H, *J* = 4.7, 13.9 Hz), 2.70 (dd, 2H, *J* = 8.6, 13.9 Hz), 1.81−1.90 (m, 2H); ^{13}C NMR (126 MHz, $CDCl_3$) δ 173.6, 146.6, 140.1, 137.2, 136.5, 136.1, 129.2, 129.0, 128.9, 128.8, 128.2, 127.5, 127.5, 126.6, 126.4, 125.6, 65.1, 53.7, 40.5, 39.5; HRMS (ESI-TOF)$^+$ calcd for $C_{41}H_{39}N_5O_2$ (M + H)$^+$ 634.3182, found 634.3181. Anal. Calcd. for $C_{41}H_{39}N_5O_2$: C, 77.70; H, 6.20; N, 11.05. Found: C, 77.51; H, 6.35; N, 10.82.

*Crystal data for [**2**-H$_2$](H$_2$PO$_4$)$_2$:* $[C_{41}H_{41}N_5O_2](H_2PO_4)_2 \cdot 0.5(H_3PO_4) \cdot 2.33(H_2O)$, *M* = 920.79, rhombohedral, *R*3 (no. 146), *a* = 30.4865(6) Å, *c* = 12.0383(4) Å, *V* = 9689.7(4) Å^3, *Z* = 9, D_c = 1.420 g cm^{-3}, μ(Mo Kα) = 0.194 mm^{-1}, *T* = 173 K, pale yellow blocks, Oxford Diffraction Xcalibur 3 diffractometer; 10055 independent measured reflections (R_{int} = 0.0270), F^2 refinement, R_1(obs) = 0.0868, wR_2(all) = 0.2622, 6751 independent observed absorption-corrected reflections [$|F_o| > 4\sigma(|F_o|)$, $2\theta_{max}$ = 58°], 676 parameters. The absolute structure of [**2**-H$_2$](H$_2$PO$_4$)$_2$ was determined by a combination of *R*-factor tests [R_1^+ = 0.0868, R_1^- = 0.0871] and by use of the Flack parameter [x^+ = +0.00(15), x^- = +1.11(15)]. CCDC 845873.

■ ASSOCIATED CONTENT

Supporting Information

^{1}H and ^{13}C NMR spectra, 2D NMR spectra, and mass spectra for compounds **1** and **2**; fluorescent titration spectra for compounds **1** and **2** with different acids; details of the DFT calculations; X-ray crystallographic information. This material is available free of charge via the Internet at http://pubs.acs.org

■ AUTHOR INFORMATION

Corresponding Author

*E-mail: (S.V.L.) luiss@qio.uji.es; (R.V.) r.vilar@imperial.ac.uk.

■ ACKNOWLEDGMENTS

The UK's Engineering and Physical Sciences Research Council (EPSRC) is thanked for a Leadership Fellowship to R.V. The Spanish Ministry of Science and Innovation (CTQ2009-14366-C02-01) and UJI-Bancaixa (P1-1B-2009-59) are thanked for support to S.V.L. The Spanish Ministry of Science (FPU AP2007-02562) and EU seventh Framework Program (PIIF-GA-2009-235411) are thanked for financial support to V.M.C. and D.K.K., respectively. The support of the SCIC of the UJI for the different instrumental techniques is acknowledged.

■ REFERENCES

(1) Moragues, M. E.; Martínez-Máñez, R.; Sancenón, F. *Chem. Soc. Rev.* **2011**, *40*, 2593−2643.
(2) Amendola, V.; Fabbrizzi, L.; Mosca, L. *Chem. Soc. Rev.* **2010**, *39*, 3889−3915.
(3) De Silva, A. P.; Moody, T. S.; Wright, G. D. *Analyst* **2009**, *134*, 2385−2393.
(4) Terai, T.; Nagano, T. *Curr. Opin. Chem. Biol.* **2008**, *12*, 515−521.
(5) Gibson, S. E.; Lecci, C. *Angew. Chem., Int. Ed.* **2006**, *45*, 1364−1377.
(6) Billing, J. F.; Nilsson, U. J. *J. Org. Chem.* **2005**, *70*, 4847−4850.
(7) Punna, S.; Kuzelka, J.; Wang, Q.; Finn, M. G. *Angew. Chem., Int. Ed.* **2005**, *44*, 2215−2220.
(8) Cristau, P.; Martin, M.-T.; Tran Hu Dau, M.-E.; Vors, J.-P.; Zhu, J. *Org. Lett.* **2004**, *6*, 3183−3186.
(9) Dietrich, B.; Viout, P.; Lehn, J.-M. *Macrocyclic Chemistry*; Wiley: New York, 1993.
(10) Horne, W. S.; Stout, C. D.; Ghadiri, M. R. *J. Am. Chem. Soc.* **2003**, *125*, 9372−9376.
(11) Fernandez-López, S.; Kim, H.; Choi, E.; Delgado, M.; Granja, J.; Khasanov, A.; Kraehenbuehl, K.; Long, G.; Weinberger, D.; Wilcoxen, K.; Ghadiri, M. *Nature* **2001**, *412*, 452−455.
(12) Loughlin, W. A.; Tyndall, J. D. A.; Glenn, M. P.; Fairlie, D. P. *Chem. Rev.* **2004**, *104*, 6085−6117.
(13) Reid, R. C.; Pattenden, L. K.; Tyndall, J. D. A.; Martin, J. L.; Walsh, T.; Fairlie, D. P. *J. Med. Chem.* **2004**, *47*, 1641−1651.
(14) Vögtle, F. *Cyclophane Chemistry*; Wiley: New York, 1993.
(15) Kyung, K.; Lee, D. H.; Hong, J. I.; Yoon, J. *Acc. Chem. Res.* **2009**, *42*, 23−31.
(16) Biot, C.; Buisine, E.; Rooman, M. *J. Am. Chem. Soc.* **2003**, *125*, 13988−13994.
(17) Owen, D. J.; Ornaghi, P.; Yang, J. C.; Lowe, N.; Evans, P. R.; Ballario, P.; Neuhaus, D.; Filetici, P.; Travers, A. A. *EMBO J.* **2000**, *19*, 6141−6149.
(18) Dhalluin, C.; Carlson, J. E.; Zeng, L.; He, C.; Aggarwal, A.; Zhou, M. *Nature* **1999**, *399*, 491−496.
(19) Perutz, M. F. *Philos. Trans. Phys. Sci. Eng.* **1993**, *345*, 105−112.
(20) Perutz, M. F.; Fermi, G.; Abraham, D. J.; Poyart, C.; Bursaux, E. *J. Am. Chem. Soc.* **1986**, *108*, 1064−1078.
(21) Mutihac, L.; Lee, J. H.; Kim, J. S.; Vicens, J. *Chem. Soc. Rev.* **2011**, *40*, 2777−2796.
(22) Caballero, A.; White, N. G.; Beer, P. D. *Angew. Chem., Int. Ed.* **2011**, *50*, 1845−1848.
(23) Gale, P. A. *Chem. Commun.* **2011**, *47*, 82−86.
(24) Gale, P. A. *Chem. Soc. Rev.* **2010**, *39*, 3746−3771.
(25) Joyce, L. A.; Shabbir, S. H.; Anslyn, E. V. *Chem. Soc. Rev.* **2010**, *39*, 3621−3632.
(26) Gale, P. A.; Gunnlaugsson, T. *Chem. Soc. Rev.* **2010**, *39*, 3595−3596.
(27) Jordan, L. M.; Boyle, P. D.; Sargent, A. L.; Allen, W. E. *J. Org. Chem.* **2010**, *75*, 8450−8456.
(28) Duke, R. M.; Veale, E. B.; Pfeffer, F. M.; Kruger, P. E.; Gunnlaugsson, T. *Chem. Soc. Rev.* **2010**, *39*, 3936−3953.
(29) Mullen, K. M.; Beer, P. D. *Chem. Soc. Rev.* **2009**, *38*, 1701−1713.
(30) Kubik, S. *Chem. Soc. Rev.* **2009**, *38*, 585−605.
(31) Coleman, A. W.; Perret, F.; Mousa, A.; Dupin, M.; Guo, Y.; Perron, H. *Top. Curr. Chem.* **2007**, *277*, 31−88.
(32) Bazzicalupi, C.; Bencini, A.; Bianchi, A.; Cecchi, M.; Escuder, B.; Fusi, V.; García-España, E.; Giorgi, C.; Luis, S. V.; Maccagni, G.; Marcelino, V.; Paoletti, P.; Valtancoli, B. *J. Am. Chem. Soc.* **1999**, *121*, 6807−6815.
(33) Arranz, P.; Bencini, A.; Bianchi, A.; Diaz, P.; García-España, E.; Giorgi, C.; Luis, S. V.; Querol, M.; Valtancoli, B. *J. Chem. Soc., Perkin Trans. 2* **2001**, 1765−1770.
(34) Aguilar, J. A.; Descalzo, A. B.; Díaz, P.; Fusi, V.; García-España, E.; Luis, S. V.; Micheloni, M.; Ramírez, J. A.; Romani, P.; Soriano. *J. Chem. Soc., Perkin Trans. 2* **2000**, 1187−1192.
(35) Burguete, M. I.; García-España, E.; López-Diago, L.; Luis, S. V.; Miravet, J.; Sroczynski, D. *Org. Biomol. Chem.* **2007**, *5*, 1935−1944.
(36) Granzhan, A.; Largy, E.; Saettel, N.; Teulade-Fichou, M. *Chem.—Eur. J.* **2010**, *16*, 878−889.
(37) Laronze-Cochard, M.; Kim, Y.-M.; Brassart, B.; Riou, J.-F.; Laronze, J.-Y.; Sapi, J. *Eur. J. Med. Chem.* **2009**, *44*, 3880−3888.
(38) Kim, S. K.; Seo, D.; Han, S. J.; Son, G.; Lee, I.-J.; Lee, C.; Lee, K. D.; Yoon, J. *Tetrahedron* **2008**, *64*, 6402−6405.
(39) Burguete, M. I.; Galindo, F.; Izquierdo, M. A.; O'Connor, J.-E.; Herrera, G.; Luis, S. V.; Vigara, L. *Eur. J. Org. Chem.* **2010**, *31*, 5967−5979.
(40) Alfonso, I.; Bolte, M.; Bru, M.; Burguete, M. I.; Luis, S. V.; Vicent, C. *Org. Biomol. Chem.* **2010**, *8*, 1329−1339.
(41) Bru, M.; Alfonso, I.; Burguete, M. I.; Luis, S. V. *Angew. Chem.,Int. Ed.* **2006**, *45*, 6155−6159.
(42) Galindo, F.; Burguete, M. I.; Vigara, L.; Luis, S. V.; Russell, D. A.; Kabir, N.; Gavrilovic, J. *Angew. Chem., Int. Ed.* **2005**, *44*, 6504−6508.
(43) Alfonso, I.; Burguete, M. I.; Galindo, F.; Luis, S. V.; Vigara, L. *J. Org. Chem.* **2009**, *74*, 6130−6142.
(44) Alfonso, I.; Burguete, M. I.; Luis, S. V. *J. Org. Chem.* **2006**, *71*, 2242−2250.
(45) Alfonso, I. *Mini-Rev. Org. Chem.* **2008**, *5*, 33−46.
(46) Kang, S.; Begum, R.; Bowman-James, K. *Angew. Chem., Int. Ed.* **2006**, *45*, 7882−7894.
(47) *Modern Supramolecular Chemistry: Strategies for Macrocycle Synthesis*; Diederich, F., Stang, P., Tykwinski, R. R., Eds.; Wiley-VCH: Weinheim, 2008.
(48) *Template Synthesis of Macrocyclic Compounds*; Gerbeleu, N. V., Arion, V. B., Burgess, J., Eds.; Wiley-VCH: Weinheim, 1999.
(49) *Macrocycle Synthesis: A Practical Approach*; Parker, D., Eds.; Oxford University Press: Oxford, 1996.
(50) Busch, D. H.; Vance, A. L.; Kolchinski, G. In *Comprehensive Supramolecular Chemistry*; Lehn, J. M., Ed.; Elsevier Science: New York, 1996; Vol. *9*.
(51) *Comprehensive Supramolecular Chemistry*; Atwood, J. L., Davies, J. E. D., MacNicol, D. D., Vogtle, F. Eds.; Pergamon: Oxford, 1996; Vol. *11*.
(52) Hess, F. K; Stewart, P. B *J. Med. Chem.* **1975**, *18*, 320−321.
(53) Becerril, J.; Bolte, M.; Burguete, M.; Galindo, F.; García-España, E.; Luis, S.; Miravet, J. *J. Am. Chem. Soc.* **2003**, *125*, 6677−6686.
(54) Bru, M.; Alfonso, I.; Bolte, M.; Burguete, M. I.; Luis, S. V. *Chem. Commun.* **2011**, *47*, 283−285.

(55) Alfonso, I.; Bolte, M.; Bru, M.; Burguete, M. I.; Luis, S. V.; Rubio, J. *J. Am. Chem. Soc.* **2008**, *130*, 6137−6144.
(56) Bru, M.; Alfonso, I.; Burguete, M. I.; Luis, S. V. *Tetrahedron Lett.* **2005**, *46*, 7781−7785.
(57) Martí-Centelles, V; Burguete, M. I.; Luis, S. V. *Chem.—Eur. J.* **2011**, accepted manuscript chem.201101416.
(58) *Handbook of Photochemistry*; Murov, S. L., Ed.; Marcel Dekker: New York, 1973.
(59) Beeren, S. R.; Sanders, J. K. M. *J. Am. Chem. Soc.* **2011**, *133*, 3804−3807.
(60) Blažek, V.; Bregović, N.; Mlinarić-Majerski, K.; Basarić, N. *Tetrahedron* **2011**, *67*, 3846−3857.
(61) Ghosh, K.; Kar, D. *Beilstein J. Org. Chem.* **2011**, *7*, 254−264.
(62) Joseph, R.; Chinta, J. P.; Rao, C. P. *Inorg. Chem.* **2011**, *50*, 7050−7058.
(63) Bazzicalupi, C.; Bencini, A.; Giorgi, C.; Valtancoli, B.; Lippolis, V.; Perra, A. *Inorg. Chem.* **2011**, *50*, 7202−7216.
(64) Arranz, P.; Bianchi, A.; Cuesta, R.; Giorgi, C.; Godino, M. L.; Gutiérrez, M. D.; López, R.; Santiago, A. *Inorg. Chem.* **2010**, *49*, 9321−9332.
(65) Jia, C.; Wu, B.; Li, S.; Yang, Z.; Zhao, Q.; Liang, J.; Li, Q.-S.; Yang, X.-J. *Chem. Commun.* **2010**, *46*, 5376−5378.
(66) Curiel, D.; Espinosa, A.; Más-Montoya, M.; Sánchez, G.; Tárraga, A.; Molina, P. *Chem, Commun.* **2009**, *48*, 7539−7541.
(67) Engblom, S. O. *Biosens. Bioelectron.* **1998**, *13*, 981−994.
(68) *Principles of Fluorescence Spectroscopy*, Lakowicz, J. R., Ed.; Springer: Berlin, 2006.
(69) Huh, Y.; Lee, J.-G.; McPhail, D. C.; Kim, K. *J. Solution Chem.* **1993**, *22*, 651−661.
(70) Kasama, K.; Klkuchi, K.; Yamamoto, S.; Uji-Ie, K.; Nishida, Y.; Kokubum, H. *J. Phys. Chem.* **1981**, *85*, 1291−1296.
(71) Kasama, K.; Klkuchi, K.; Nishida, Y.; Kokubum, H. *J. Phys. Chem.* **1981**, *85*, 4148−4153.
(72) Diverdi, L. A.; Topp, M. R. *J. Phys. Chem.* **1984**, *88*, 3447−3451.
(73) Adams, M. J.; Highfield, J. G.; Kirkbright, G. F. *Anal. Chem.* **1977**, *49*, 1850−1852.
(74) Burguete, M. I.; Clares, M. P.; García-España, E.; Luis, S. V.; Querol, M.; Martí-Centelles, V. *Tetrahedron* **2011**, *67*, 4655−4663.
(75) The N−H hydrogen atoms in the structure of $[\mathbf{2}\text{-}H_2](H_2PO_4)_2$ could not be located. Inferring the location of these hydrogen atoms by considering heteroatom distances is further complicated by disorder and partial occupancy issues for the cocrystallised PO_4 units and water molecules. Furthermore, the acridinyl unit portion of the macrocycle was itself found to be disordered. See the Supporting Information for more details.
(76) Procedure adapted from ref 42.
(77) *Spartan '08 (build 132)*; Wavefunction, Inc.: Irvine, CA, 2009.
(78) Gaussian 03, Revision D.02: Frisch, M. J.; Trucks, G. W.; Schlegel, H. B.; Scuseria, G. E.; Robb, M. A.; Cheeseman, J. R.; Montgomery, J. A., Jr.; Vreven, T.; Kudin, K. N.; Burant, J. C.; Millam, J. M.; Iyengar, S. S.; Tomasi, J.; Barone, V.; Mennucci, B.; Cossi, M.; Scalmani, G.; Rega, N.; Petersson, G. A.; Nakatsuji, H.; Hada, M.; Ehara, M.; Toyota, K.; Fukuda, R.; Hasegawa, J.; Ishida, M.; Nakajima, T.; Honda, Y.; Kitao, O.; Nakai, H.; Klene, M.; Li, X.; Knox, J. E.; Hratchian, H. P.; Cross, J. B.; Bakken, V.; Adamo, C.; Jaramillo, J.; Gomperts, R.; Stratmann, R. E.; Yazyev, O.; Austin, A. J.; Cammi, R.; Pomelli, C.; Ochterski, J. W.; Ayala, P. Y.; Morokuma, K.; Voth, G. A.; Salvador, P.; Dannenberg, J. J.; Zakrzewski, V. G.; Dapprich, S.; Daniels, A. D.; Strain, M. C.; Farkas, O.; Malick, D. K.; Rabuck, A. D.; Raghavachari, K.; Foresman, J. B.; Ortiz, J. V.; Cui, Q.; Baboul, A. G.; Clifford, S.; Cioslowski, J.; Stefanov, B. B.; Liu, G.; Liashenko, A.; Piskorz, P.; Komaromi, I.; Martin, R. L.; Fox, D. J.; Keith, T.; Al-Laham, M. A.; Peng, C. Y.; Nanayakkara, A.; Challacombe, M.; Gill, P. M. W.; Johnson, B.; Chen, W.; Wong, M. W.; Gonzalez, C.; Pople, J. A. Gaussian, Inc., Wallingford, CT, 2004.
(79) Gaussian 09, Revision B.01: Frisch, M. J.; Trucks, G. W.; Schlegel, H. B.; Scuseria, G. E.; Robb, M. A.; Cheeseman, J. R.; Scalmani, G.; Barone, V.; Mennucci, B.; Petersson, G. A.; Nakatsuji, H.; Caricato, M.; Li, X.; Hratchian, H. P.; Izmaylov, A. F.; Bloino, J.; Zheng, G.; Sonnenberg, J. L.; Hada, M.; Ehara, M.; Toyota, K.; Fukuda, R.; Hasegawa, J.; Ishida, M.; Nakajima, T.; Honda, Y.; Kitao, O.; Nakai, H.; Vreven, T.; Montgomery, J. A., Jr.; Peralta, J. E.; Ogliaro, F.; Bearpark, M.; Heyd, J. J.; Brothers, E.; Kudin, K. N.; Staroverov, V. N.; Kobayashi, R.; Normand, J.; Raghavachari, K.; Rendell, A.; Burant, J. C.; Iyengar, S. S.; Tomasi, J.; Cossi, M.; Rega, N.; Millam, J. M.; Klene, M.; Knox, J. E.; Cross, J. B.; Bakken, V.; Adamo, C.; Jaramillo, J.; Gomperts, R.; Stratmann, R. E.; Yazyev, O.; Austin, A. J.; Cammi, R.; Pomelli, C.; Ochterski, J. W.; Martin, R. L.; Morokuma, K.; Zakrzewski, V. G.; Voth, G. A.; Salvador, P.; Dannenberg, J. J.; Dapprich, S.; Daniels, A. D.; Farkas, O.; Foresman, J. B.; Ortiz, J. V.; Cioslowski, J.; Fox, D. J. Gaussian, Inc.: Wallingford, CT, 2009.